

Zhiling Huoxue Tongyu capsule inhibits rabbit model of hyperlipidemia and atherosclerosis through NF- κ B/NLRP3 signaling pathway

Mengnan Liu^{a,b,1,*}, Raoqiong Wang^{a,b,1}, Mingtai Chen^{b,c,1}, Zhongjing Hu^a, Mei Han^a, Maryam Mazhar^a, Jinyi Xue^d, Yuan Zou^d, Qibiao Wu^{b,e,**}, Sijin Yang^{a,b,***}

^a National Traditional Chinese Medicine Clinical Research Base and Department of Cardiovascular Medicine, the Affiliated Traditional Chinese Medicine Hospital, Southwest Medical University, Luzhou, Sichuan, PR China

^b Faculty of Chinese Medicine and State Key Laboratory of Quality Research in Chinese Medicine, Macau University of Science and Technology, Macau SAR, PR China

^c Department of Cardiovascular Disease, Shenzhen Traditional Chinese Medicine Hospital, Shenzhen, Guangdong, PR China

^d School of Integrative Traditional Chinese and Western Medicine, Southwest Medical University, Luzhou, Sichuan, PR China

^e Guangdong-Hong Kong-Macao Joint Laboratory for Contaminants Exposure and Health, Guangzhou, Guangdong, PR China

ARTICLE INFO

Keywords:

Inflammation
Pyroptosis
Atherosclerosis
Zhiling Huoxue Tongyu capsule
Traditional Chinese medicine

ABSTRACT

Objective: Zhiling Huoxue Tongyu capsule (ZL) is a Chinese patent medicine for treating cardio-cerebral diseases. However, the pharmacological mechanism by which it regulates blood lipids and treats atherosclerosis (AS) is unclear. Therefore, the purpose of this study is to explore the mechanism of ZL inhibiting hyperlipidemia and treating AS through NF- κ B/NLRP3 signaling pathway.

Methods: Fifty New Zealand white rabbits were divided into control, model, model + ZL (3.12 g/kg/d, i.g.), model + atorvastatin (0.51 mg/kg/d, i.g.), and model + ZL + atorvastatin groups. Except for the control group, all other groups underwent carotid intima air drying and received a high-fat diet for 28 days to establish hyperlipidemia AS model, and drug treatment was given for the same period of time after modeling. Pathological changes and blood lipids were detected, NF- κ B/NLRP3-related protein or gene expression levels were analyzed in carotid tissue.

Results: ZL significantly reduced blood lipids and delayed the progression of AS. TC, TG, and LDL-C were decreased while HDL-C was increased in blood, IMT thickening and plaque formation of carotid arteries were inhibited, VRI was alleviated, and pathological features were improved. NF- κ B, NLRP3 and IL-1 β in the carotid artery were significantly down-regulated after intervention with ZL. RT-PCR and western blot analysis showed that NF- κ B (p-NF- κ B), NLRP3, caspase-1, IL-1 β and IL-18 were significantly downregulated by ZL.

* Corresponding author. National Traditional Chinese Medicine Clinical Research Base and Department of Cardiovascular Medicine, the Affiliated Traditional Chinese Medicine Hospital, Southwest Medical University, Luzhou, Sichuan, PR China.

** Corresponding author. Faculty of Chinese Medicine and State Key Laboratory of Quality Research in Chinese Medicine, Macau University of Science and Technology, Macau SAR, PR China.

*** Corresponding author. National Traditional Chinese Medicine Clinical Research Base and Department of Cardiovascular Medicine, the Affiliated Traditional Chinese Medicine Hospital, Southwest Medical University, Luzhou, Sichuan, PR China.

E-mail addresses: liumengnan@swmu.edu.cn (M. Liu), qbwu@must.edu.mo (Q. Wu), ysjimm@sina.com (S. Yang).

¹ Mengnan Liu, Raoqiong Wang and Mingtai Chen contributed equally to this work.

<https://doi.org/10.1016/j.heliyon.2023.e20026>

Received 25 June 2023; Received in revised form 20 August 2023; Accepted 8 September 2023

Available online 9 September 2023

2405-8440/© 2023 Published by Elsevier Ltd.

This is an open access article under the CC BY-NC-ND license

(<http://creativecommons.org/licenses/by-nc-nd/4.0/>).

Conclusions: ZL can be used effectively as adjuvant therapy for hyperlipidemia and AS, combining it with atorvastatin yielded more optimized efficacy, but its anti-inflammatory and pharmacological mechanisms of inhibiting pyroptosis should be studied further.

1. Introduction

Atherosclerosis (AS) is a major risk factor for cardio-cerebrovascular event [1]. The morbidity and mortality rates of cardiovascular and cerebrovascular diseases caused by AS are gradually increasing worldwide, and the age of onset is decreasing [2]. The carotid artery is the most vulnerable part in the occurrence of AS, and reflects the systemic arterial disease; therefore, carotid artery lesions are often associated with cardiovascular and cerebrovascular events [3]. The mechanism of AS is complex, and is mainly attributed to vascular endothelial injury, abnormal lipid metabolism, and hemodynamic changes among others. All these factors jointly wreak havoc on the vascular wall, eventually leading to chronic inflammation of the vessel and consequently causing AS [4]. Therefore, carotid artery lesions are often associated with cardiovascular and cerebrovascular events.

Pyroptosis has been widely studied as programmed cell death [5]. Nucleotide-binding oligomerization domain-like receptor protein 3 (NLRP3) is a member of the NLRP protein family, and can identify endogenous damage-associated molecular patterns (DAMPs) and cause inflammatory responses. NLRP3 inflammasome is involved in the inflammatory process of nuclear factor kappa-B (NF- κ B)-mediated diseases, NLRP3 activation promotes the secretion of inflammatory factors such as interleukins, and vascular endothelial damage caused by inflammation leads to the occurrence of AS [6,7]. From the perspective of dyslipidemia, oxidized low-density lipoprotein (ox-LDL) promotes cholesterol crystallization, and as an endogenous signaling molecule, it promotes the maturation and secretion of inflammatory factors, and mediates the early inflammatory response in AS [8,9]. Therefore, vascular inflammation and dyslipidemia are often regarded as common pathological factors in AS.

Lipid regulation, and anti-inflammatory and antithrombotic therapy are the main modes of treatment for AS [10,11]. In recent years, numerous non-clinical and clinical studies have shown that traditional Chinese medicine (TCM) can yield satisfactory efficacy in the treatment of AS without significant adverse reactions [12,13]. Zhilong Huoxue Tongyu capsule (ZL) is a TCM preparation for the treatment of cardiovascular and cerebrovascular diseases, and is composed of *Astragalus membranaceus* (Fisch.) Bunge. Fabaceae, *Cinnamomum cassia* Presl. Lauraceae, *Sargentodoxa cuneata* (Oliv.) Rehd.et Wils. Lardizabalaceae, *Pheretima Aspergillum* (E. Perrier) Megascolecidae, and *Hirudo nipponica* Whitman Hirudideae. Previous studies have shown that it can regulate the release of inflammatory factors, protect vascular endothelium, and promote angiogenesis [14,15]. These five components provide a rich pharmacodynamic material basis. In particular, ZL ameliorated lipid-induced endothelial cell pyroptosis [16]. The aforementioned medicines can resist AS, thereby reducing the risk of cardiovascular and cerebrovascular diseases. More importantly, the long-term toxicity of ZL was observed using the maximum tolerated dose (81.6 g/kg/d) in mice, indicating no obvious effect on the physiological function and obvious long-term toxic effects [6,7].

The treatment of AS by inhibiting the inflammatory response is a focal topic in TCM research [17]. Presently, the mechanism of the inflammatory response caused by abnormal lipid metabolism and endothelial injury in the occurrence of AS has not been fully elucidated [2]. Therefore, in this study, a hyperlipidemia carotid AS rabbit model was established, and ZL and atorvastatin were used separately or jointly for intervention. We determined its preliminary pharmacological mechanism and therapeutic effect by targeting the NF- κ B/NLRP3 signaling pathway, and further determined the efficacy of solely using ZL or combining it with atorvastatin in this model.

2. Methods

2.1. Animals, drugs and reagents

Fifty adult clean-grade male New Zealand white rabbits, weighing 2.0 ± 0.4 kg, were maintained in the Animal Experiment Center of Southwest Medical University (Certification No. SYXK Chuan 2018-065), with a 12 h dark/light cycle, room temperature ranging from 19 to 22 °C, and humidity ranging from 40 to 60%. Animal experimental procedures were approved by the Animal Research

Table 1
Details of antibodies.

primary antibody	Manufacturer	Catalog	Application
p-NF κ B	St John's Laboratory, UK	stj28018	WB
NF κ B	Aviva Systems Biology, USA	arp38197_p050	WB
NLRP3	Aviva Systems Biology, USA	arp63297_p050	WB
Caspase-1	Aviva Systems Biology, USA	arp58983_p050	WB
IL-1 β	Aviva Systems Biology, USA	arp54323_p050	WB
IL-18	Cloud-Clone, Houston, USA	paa064rb51	WB
NF κ B	Affinity Biosciences, USA	AF5006	IF
NLRP3	Affinity Biosciences, USA	DF7438	IF
IL-1 β	Affinity Biosciences, USA	AF5103	IHC

Committee of Southwest Medical University (Approval Number. SWMU20220072). All experimental procedures were performed in accordance with the National Institute of Health Guide for the Care and Use of Laboratory Animals. Zhilong Huoxue Tongyu capsule (Med-drug permit no. Chuan Z20070528; Patent number 200810147774.1) was provided by the Preparation Room for TCM at the Affiliated Hospital of TCM, Southwest Medical University. The preparation method and composition analysis of the drug have been discussed in a previous study [15]. Atorvastatin (Med-drug permit no. H20093819) was purchased from Beijing Jialin Pharmaceutical Co., Ltd. The feed was provided by the Animal Experiment Center of Southwest Medical University, and the high-fat feed consisted of 96% normal feed (Dashuo Co., Ltd, Cat. No. ds0025), 2% cholesterol (Solarbio Co., Ltd, Cat. No. C8280), and 2% lard (Sigma Co., Ltd, Cat. No. L0657); all feeds were stored at 4 °C. The specific information of antibodies (p-NF- κ B, NF- κ B, NLRP3, caspase-1, IL-1 β , IL-18, β -actin.) is presented in Table 1. RNA extraction (Cat. No. NPK-201F), reverse transcription (Cat. No. FSQ-201), and reaction reagents (Cat. No. KMM-101) were purchased from TOYOBO (Shanghai) Biotech Co., Ltd. The primers were designed and provided by Sangon Biotech (Shanghai) Co., Ltd. BCA protein concentration assay kit (Cat. No. P0012S) and protein lysis buffer (Cat. No. L00025) were purchased from Beyotime Biotechnology Co., Ltd. Hematoxylin and eosin (H&E) staining kit (Cat. No. G1120) and Masson staining kit (Cat. No. G1340) were purchased from Beijing Solarbio Science & Technology Co., Ltd.

2.2. Animal model

High fat diet (96% common feed, 2% cholesterol, 2% lard) with carotid intima air drying was used to establish the rabbit model of hyperlipidemia and AS [18,19]. The experimental animals were subjected to a 12 h fast before operation, and provided with unlimited drinking water. The rabbits were injected with 846 anesthetic mixture (Approval Number. LuYaoZi (2010) 700315822, a compound preparation of 4-xyridinethiazole, ethylenediaminetetraacetic acid, dihydroetorphine hydrochloride, and haloperidol) 0.2 mL/kg to anesthetize, using the dosage stipulated in the instructions. After each neck was depilated, cleaned, and sterilized, a median neck skin incision, approximately 2.5 cm in length, was made, and the left common carotid artery was separated horizontally above the thyroid cartilage. Arterial clips were used to block blood flow on both sides. A 4.5-gauge scalp needle was used to puncture the longitudinal axis of the blood vessel and entered in both ends of the blocked blood vessel, and the blood in the lumen was replaced with normal saline. For the subsequent 5 min, a dry air flow of 250 mL/min was used to dry the endothelium, after which the carotid artery was refilled with saline. At this point the arterial clip was removed to restore blood flow to the carotid artery. The puncture point was compressed for 2–3 min to stop the bleeding, and then the skin was sutured and bandaged. Gentamicin was used intramuscularly after surgery to prevent infection. Generally speaking, 14 d after the operation, the carotid intima-media of the animal model will show significant plaque proliferation. With the feeding of high-fat diet, the plaque proliferation will be faster and closer to the natural growth of human carotid atherosclerotic plaque. The development of the model was evaluated by carotid artery thickening and pathological staining.

2.3. Experimental grouping

After 1 week of adaptive feeding, all the rabbits were randomly divided into 5 groups: (1) control group, (2) model group, (3) model + ZL group, (4) model + atorvastatin group, and (5) model + ZL + atorvastatin group, and provided with unlimited drinking water, except for the control group, which received basal feed. The rest of the groups were fed a constant high-fat diet to provide 150 g of feed per animal per day.

After the successful development of a model, the animals in all treatment groups received drug treatment at 8:00 a.m. daily for 4 weeks. The ZL dosage was 4.8 g/d for adults, and 3.12 g/kg/d for animals, which is 6 times the adult dosage refer to our previous research [20]. The model + atorvastatin group received a dose of 0.51 mg/kg/d, which was 3 times that of the clinical adult dosage. The aforementioned doses were converted according to the doses of the humans and animals. According to previous research data, the above dose does not cause toxic damage to experimental animals. Both the ZL and atorvastatin were thoroughly dissolved in drinking water, and gavaged at a volume of 4 mL/kg.

2.4. General physical appearance, lipid profile analysis and ultrasound diagnosis

During the experiment, the rabbits were observed daily for poor healing and wound infection. The weight measurement was also recorded every week. The ultrasound diagnostic system (ACUSON OXAMA2, Siemens, Germany) was used to observe the carotid artery lesions in rabbits, with observation time points starting from the 1st day of modeling, followed by the 14th, 21st, and 28th days. The observation indicators of intima-media thickness (IMT) and vascular resistance index (VRI) were used. $VRI = [\text{peak systolic flow rate (A)} - \text{diastolic flow rate (B)}] / \text{peak systolic flow rate (A)}$, all values were automatically calculated by the system.

After ultrasound diagnosis, 5 mL of blood was collected from the ear vein and placed in an anticoagulant tube, centrifuged at 4 °C and 3000 rpm/min for 10 min to separate serum and detect total cholesterol (TC), triglyceride (TG), low-density lipoprotein cholesterol (LDL-C), and high-density lipoprotein cholesterol (HDL-C), the samples were analyzed using the automatic biochemical analyzer (cobas8000 C702, Roche, Switzerland).

2.5. Sample collection

On the 28th day of the experiment, the rabbits were sacrificed by intra-arterial injection of air after the aforementioned tests were completed. The skin of the neck was cut open, the right common carotid artery was exposed, and the 3 cm-long diseased artery was

taken out and cut evenly. The arteries were divided into 3 sections, one of which was fixed in 4% paraformaldehyde, and the rest were frozen at -80°C for extraction of RNA and protein.

2.6. Pathological staining

H&E and Masson staining were performed, according to the kit instructions and all the steps are as follows. For H&E staining, the carotid tissues fixed by 4% paraformaldehyde were embedded in paraffin, and paraffin sections were used for machine making $4\ \mu\text{m}$'s section. The slices were placed in an oven at 56°C for 1 h, and the dried paraffin slices were dewaxed with conventional xylene, and then subjected to downward gradient ethanol hydration, washed with distilled water, added with hematoxylin for dyeing for 10 min, and then washed with running water to remove the hematoxylin dye solution. 1% hydrochloric acid ethanol was used to fade, when the slices were found to be red and light, they were put into tap water to restore the blue color. The slices were dyed with eosin for 1 min, washed with running water, dehydrated and dried with gradient alcohol. Xylene was used for dehydration, after dropping neutral gum for sealing treatment, the microscope (BA210LED, Motic, China) was used to take pictures. For Masson staining, $4\ \mu\text{m}$ sections of the carotid tissues were routinely deparaffinized in xylene and stained for 5 min in Weigert's iron hematoxylin staining solution. The acid ethanol differentiation solution was treated for 5 s and washed with tap water. Masson's blue liquor is returned to blue for 5 min, washed with tap water, and then washed with distilled water for 1 min. The stains were stained with Ponceau fuchsin staining solution for 5 min, washed with phosphomolybdic acid solution for 1 min, and washed with aniline blue staining solution for 1 min, after the completion of each of the above steps, it was necessary to put in a weak acid working solution for 1 min. After all the above work was completed, the slices were dehydrated by gradient alcohol, transparent by xylene, sealed by dropping neutral gum, and photographed using a microscope.

2.7. Immunohistochemistry

Immunohistochemistry was used to observe the expression of inflammatory factor, (IL-1 β) in myocardial tissue. $4\ \mu\text{m}$ sections were routinely deparaffinized with xylene, hydrated with descending gradient ethanol, washed with distilled water, incubated with 3% H_2O_2 drip for 10 min at room temperature, washed 3 times with PBS for 3 min each time, blocked with normal goat immune serum drip, incubated for 10 min at room temperature and then added with primary antibody drip (dilution 1:200) in the refrigerator at 4°C overnight. The following day, each section was added dropfold with secondary antibody (dilution 1:200), incubated for 10 min at room temperature, and washed again. DAB was used for color development and the reaction time was controlled under the microscope. Finally, the stained slides were sealed with neutral gum drops and observed under a bright field microscope and images were captured. The quantification analysis for positively stained areas was performed using Image Pro 6.0 software.

2.8. Immunofluorescence

Paraffin sections were dewaxed and antigen was retrieved; then 3% hydrogen peroxide was added to inactivate endogenous enzymes. After washing, goat serum was used for blocking, followed by incubation with NF- κB primary antibody (dilution 1:100) at 4°C overnight. The following day, the primary antibody was recovered and the slides were washed with PBS 3X. Subsequently, the slides were incubated with fluorescent secondary antibody (cy3)-labeled goat anti-mouse IgG (dilution 1:100) for 1 h at room temperature in the dark. After being recovered and washed, another primary antibody anti-NLRP3 was used for incubation following the aforementioned steps. Fluorescence (FITC)-labeled goat anti-IgG (dilution 1:100) was used for secondary antibody incubation. Finally, the anti-fluorescence quencher containing DAPI was added. Upright fluorescence microscope (BA210LED, Nikon, Japan) was used to observe the slides and to acquire images. The mean gray value was also calculated using Image Pro 6.0 software.

2.9. RT-PCR

Total RNA from arterial tissue was extracted according to the manufacturer's instructions. After reverse transcription and amplification, fluorescence quantitative PCR instrument (LightCycler 480II, Roche, Switzerland) was used for routine melting curve analysis to determine the Ct value and GAPDH was used as an internal reference for control, and the relative expression level of target mRNA was quantified using the $2^{-\Delta\Delta\text{Ct}}$ method. The primer sequences of NF- κB , NLRP3, caspase-1, IL-1 β , IL-18, and GAPDH were listed in Table 2.

Table 2
The primer sequence for RT-PCR.

Primer's name	Forward sequence 5'-3'	Reverse sequence 5'-3'
NF- κB	TGCCATTGTCTTCAAACTCCA	ACGGTAACAG AAGTTTGTAGGT
NLRP3	CCACTTCCCAGAATCGAGA	TGGACGTGAGACAGGAGTTC
Caspase-1	CAAGTCTCAAGCITTTGCCCG	TAATGAGGGCAAGACGGGGT
IL-1 β	GAAATCCTTGGTGTGTCTGGC	CITTAGGAACCAACACAG ACCG
IL-18	GCATCAACTTTGTGGGAATG	CGGTTCAAGCTTGCCAAA
GAPDH	GACATCAAGAAGGTGGTGAAGC	CAGCATCGAAGGTAGAGGAGTG

2.10. Western blot analysis

Protein extraction of arterial tissue was carried out on ice. The concentration of the protein sample was determined using the BCA method, and the protein loading buffer was added via denaturation at 100 °C for 10 min. 10% SDS-PAGE separation and concentration gels were configured according to the SDS-PAGE gel configuration kit instructions (Epizyme Co., Ltd, Cat. No. PG212). The denatured protein samples were added to the gel according to the loading order, and the pre-dyed protein marker and samples were loaded after adding an appropriate amount of running buffer pre-cooled in advance. Electrophoresis was carried out at 150 V for 60 min. The activated PVDF membrane (Millipore Co., Ltd, Cat. No. ISEQ00010) and gel were used to make the “sandwich” structure of the membrane transfer. The membrane was transferred at 300 mA constant flow and the transfer time was set according to the protein size. The TBST solution containing 5% bovine serum albumin was used for blocking, then the primary antibodies (1:1000) were added and incubated at 4 °C overnight. After washing the following day, the secondary antibody (1:5000) was added and incubated at room temperature for 2 h. After washing again, the ECL chemiluminescence solution (Affinity Co., Ltd, Cat. No. KF8001) was added to cover the target band position and the Chemiluminescence imaging system (ChemiScope 6200, Clinx, China) was used to acquire images and the grayscale values of the bands were analyzed using ImageJ software.

2.11. Statistical analysis

GraphPad Prism Ver 9.0 was used to perform statistical analysis on the results. The data were expressed as mean \pm standard deviation. Two-way or one-way ANOVA analysis of variance was used in statistics. The LSD *t*-test was used for pairwise comparisons between groups, and $p < 0.05$ was considered to be statistically significant.

3. Results

3.1. ZL improves AS in rabbits

Before the animals were sacrificed, the general health conditions were recorded. All the animals were normal and their autonomous

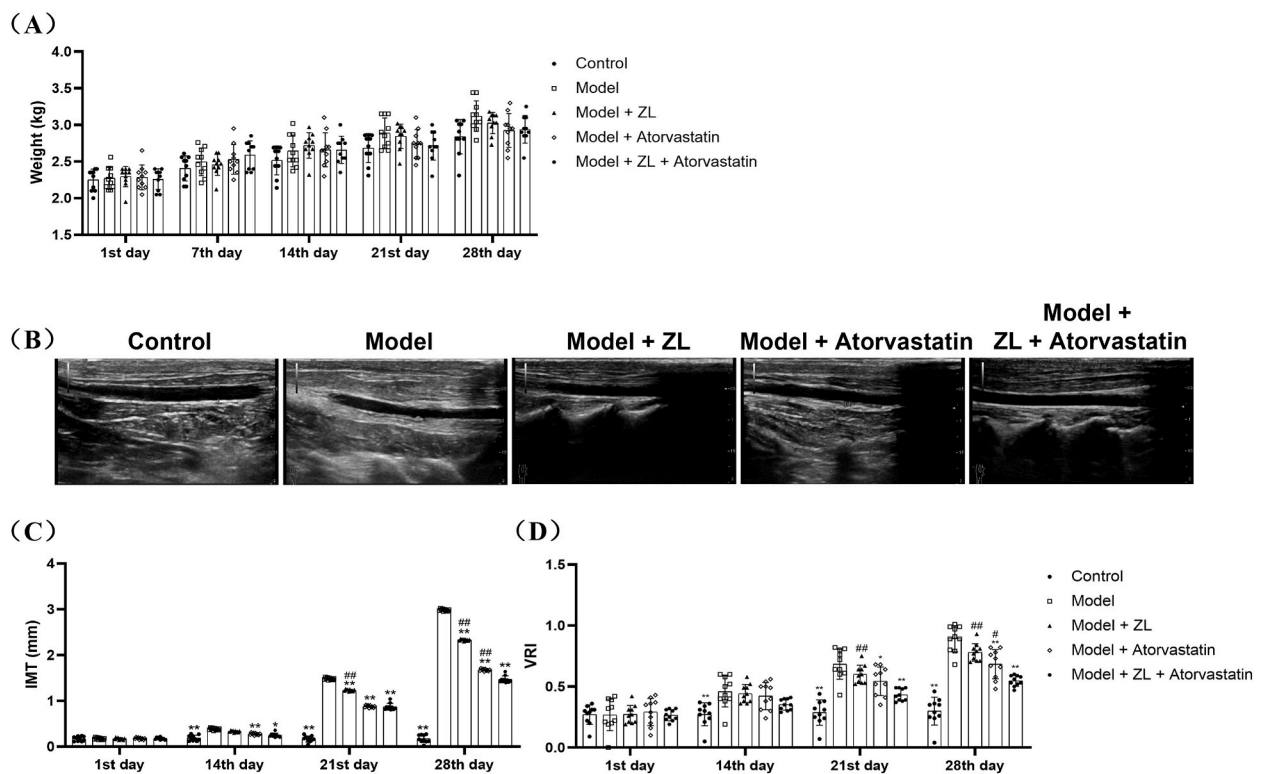


Fig. 1. ZL improves the AS in rabbits. (A) The weight changes of all experimental animals within 28 days, and the comparison of weight among the groups was found to have no statistical significance. The line chart showed the trend of weight growth, and bars represent the mean \pm SD, $n = 10$. (B) Original image of carotid artery detected using color Doppler ultrasound. Doppler ultrasound demonstrated the changes of (C) IMT and (D) VRI, and the measurements data on the 28th day were used for statistical analysis. Bars represent the mean \pm SD, $n = 10$. $*p < 0.01$ compared to the model group, $##p < 0.01$ compared to the model + ZL + atorvastatin group.

activities, diet, and drinking water were not restricted. There were no signs of anorexia, weight loss, drug side effects, and sudden acute death in each group. The body weight of experimental rabbits in each group increased physiologically, and the average body weight comparison between each group was not statistically significant ($p > 0.05$), as shown in Fig. 1A.

Color Doppler ultrasound data from the 1st to the 28th day showed that the parameters of IMT and VRI in the control group did not change significantly throughout the experiment, but changed in a time-dependent manner after high-fat diet feeding and surgical intervention, indicating that the luminal area of the carotid arteries continued to shrink, and the IMT and VRI continued to increase. Finally, on the 28th day of testing, all these indicators peaked, as shown in Fig. 1 (B-D). The results showed that ZL or atorvastatin treatment only could effectively improve the carotid lesions ($p < 0.05$) compared to the model group, whereas ZL combined with atorvastatin showed more optimized therapeutic effects ($p < 0.05$), as shown in Fig. 1B.

3.2. ZL improves blood lipid profile in hyperlipidemic rabbits

There was no significant difference among the lipid profile indexes detected in rabbits in each group at the beginning of our experiment. In the control group, the blood lipid components were maintained and there was no significant change throughout the experiment. After the model was built, the blood lipid contents of TC, TG, LDL-C, and HDL-C in serum gradually increased over time, while on the 28th day, the blood lipid indexes of each group peaked. Compared with the model group, each drug group had different degrees of therapeutic effects on all the parameters ($p < 0.05$). The use of ZL or atorvastatin treatment alone effectively reduced these indexes, while the combined use of ZL and atorvastatin better reduced TC, TG and LDL-C ($p < 0.05$), and increased HDL-C ($p < 0.05$), as shown in Fig. 2 (A-D).

3.3. ZL inhibits carotid intima-media thickening and reduces atherosclerotic plaque formation

H&E staining (Fig. 3A) showed that the endothelial cells in the control group were intact and properly arranged, closely adhering to the inner vascular elastic plate, the smooth muscle cells in the middle layer were neatly arranged, spindle-shaped or oval-shaped, and the cytoplasm was stained eosinophilic red. Various cells in the blood vessels of the model group proliferated significantly, and lipid plaques composed of a large number of foam cells were observed; these plaques were infiltrated by inflammatory cells. A thin fibrous cap with a lipid core is observed in moderate-to-severe stenotic atherosclerotic plaques, especially in the shoulder portion of the plaque showing signs of ulceration and instability. The images demonstrated carotid arterial microstructure and the morphology of the atherosclerotic plaque (indicated by black arrows), with the internal elastic plate beneath the plaques being straightened and fractured microscopically (indicated by green arrows). Masson staining (Fig. 3B) showed changes in IMT more clearly and intuitively, and the proliferation of vascular fibrotic tissues was stained blue. After treatment with ZL or atorvastatin, the proliferation of vascular intima-media in each drug group and lipid infiltration were significantly reduced, and the vascular stenosis and severity of atherosclerotic lesions were improved. Furthermore, ZL combined with atorvastatin appeared to have a more optimized curative effect.

3.4. ZL attenuates carotid vascular inflammation

We further examined the co-expression of NF- κ B and NLRP3 in rabbit carotid lesions (Fig. 4A), as well as the expression of IL-1 β (Fig. 4B). Compared with the control group, the expressions of NF- κ B, NLRP3, and IL-1 β in the carotid arteries of the rabbits in the model group were significantly increased ($p < 0.01$), which showed that during the progression of AS, inflammation-related pathways

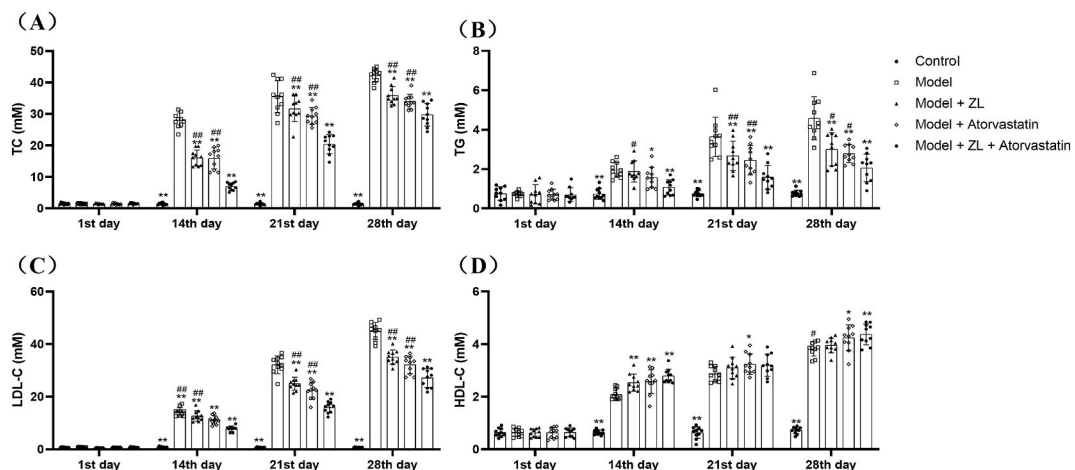


Fig. 2. ZL improved blood lipids in hyperlipidemic rabbits. The automatic biochemical analyzer was used to detect the blood lipid content in the collected blood samples, (A) TC, (B) TG, (C) LDL-C and (D) HDL-C. Bars represent the mean \pm SD, $n = 10$. * $p < 0.05$ and ** $p < 0.01$ compared to the model group, # $p < 0.05$ and ## $p < 0.01$ as compared to model + ZL + atorvastatin group.

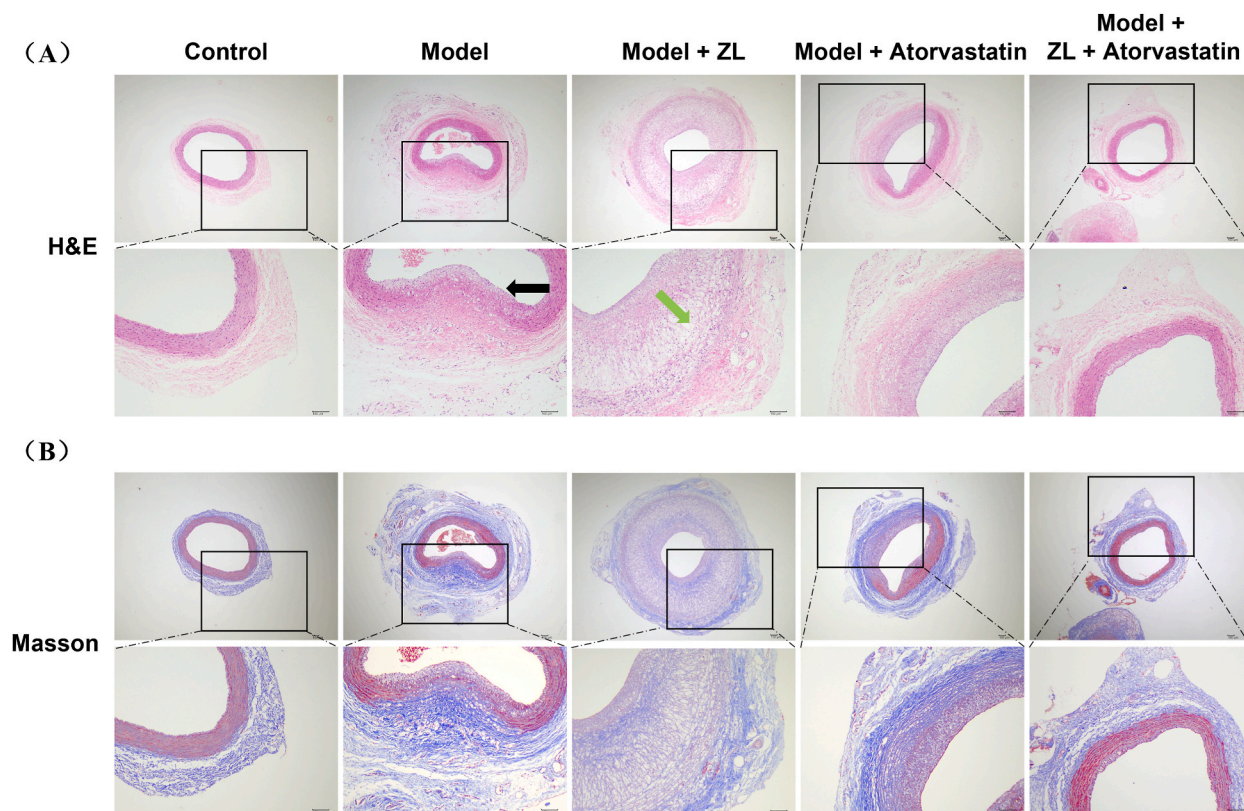


Fig. 3. ZL inhibits carotid intima-media thickening and reduces atherosclerotic plaque formation. (A) H&E staining, (B) Masson staining. Under the microscope, $40\times$ images were acquired to show histological changes throughout the vessel cross-section, with $100\times$ magnification to reveal details.

co-mediated by NF- κ B and NLRP3 were activated, and inflammatory factor IL-1 β was continuously released owing to lipid deposition in tissues and endothelial cell damage. Compared with the model group, the expressions of NF- κ B, NLRP3, and IL-1 β in the carotid tissue of each drug group decreased significantly ($p < 0.01$). ZL and atorvastatin inhibited the activation of NF- κ B/NLRP3 signaling pathway and reduced the release of inflammatory factor IL-1 β to improve AS significantly ($p < 0.05$) compared to the model group, but atorvastatin did not show a significant difference in inhibiting IL-1 β expression ($p > 0.05$). However, more optimized therapeutic effects were demonstrated in NF- κ B & NLRP3 after the combined use of drugs ($p < 0.05$), as shown in Fig. 4 (C-D).

3.5. ZL reduces the expression levels of pyroptosis-related mRNA and protein in atherosclerotic tissue

The mRNA expression levels of transcription factor NF- κ B and its downstream target genes of inflammatory factors such as NLRP3, caspase-1, IL-1 β , and IL-18 in carotid artery tissue were detected. The expressions of inflammatory factors in all lesion tissues were significantly higher than those in the control group ($p < 0.05$). After treatment, both ZL and atorvastatin significantly down-regulated the mRNA expressions of these inflammatory factors ($p < 0.05$). However, except for caspase-1, the combined treatment of the ZL and atorvastatin was more optimized than that of ZL alone ($p < 0.05$) as shown in Fig. 5A.

We also detected the protein expression of targets related to the NF- κ B/NLRP3 signaling pathway. Compared with the control group, the expressions of p-NF- κ B, NLRP3, caspase-1, IL-1 β , and IL-18 in the model group increased significantly ($p < 0.05$), indicating that a strong inflammatory reaction occurred in the lesion tissue. Compared with the model group, the ZL group significantly reduced the expressions of p-NF- κ B, NLRP3, caspase-1, IL-1 β , and IL-18, indicating that the inflammatory response was significantly inhibited. However, the combined use of ZL and atorvastatin had a more optimized effect on regulating the expression of IL-18 ($p < 0.05$) as shown in Fig. 5 (B-G).

4. Discussion

We established hyperlipidemia with carotid AS rabbit model through high fat diet plus vascular endothelium air drying. In this study, the mRNA and protein of inflammatory factors were significantly expressed in the lesion area of the carotid artery tissue of the model animals, indicating a severe inflammatory response in the atherosclerotic tissue. Lipid infiltration and vascular endothelial injury are the main causes of AS, our model simulates the formation of human atherosclerotic plaque and facilitates further exploration of the pathophysiological process of AS. With respect to treatment, we intervened the model with ZL, atorvastatin and ZL +

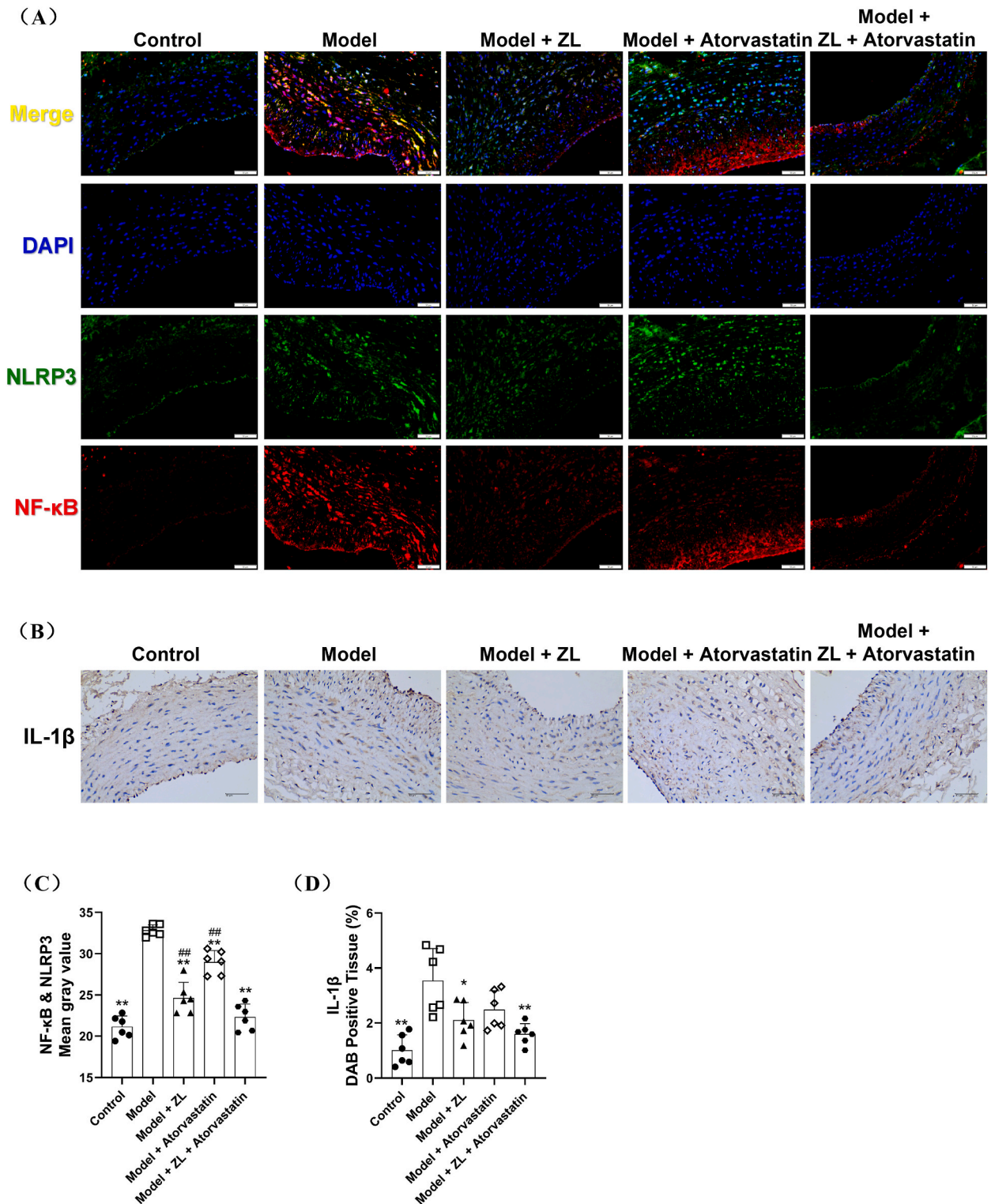


Fig. 4. ZL attenuates carotid vascular inflammation. (A) Double immunofluorescence of NF-κB and NLRP3. Atherosclerotic tissue was stained with NF-κB (green), NLRP3 (red), and DAPI (blue) to mark atherosclerotic plaques and areas of inflammation, respective changes in color in the merged figures corresponded to Red + Blue = Magenta; and Red + Green = Yellow. (B) Immunohistochemistry of IL-1β. For the above staining, we made two slices, and three fields of view ($\times 200$) were randomly selected for each slice for gray value analysis. (C) Gray value analysis of double immunofluorescence (NF-κB & NLRP3). (D) Gray value analysis of immunohistochemistry (IL-1β). Bars represent the mean \pm SD, $n = 6$. * $p < 0.05$ and ** $p < 0.01$ compared to the model group, ## $p < 0.01$ compared to the model + ZL + atorvastatin group.

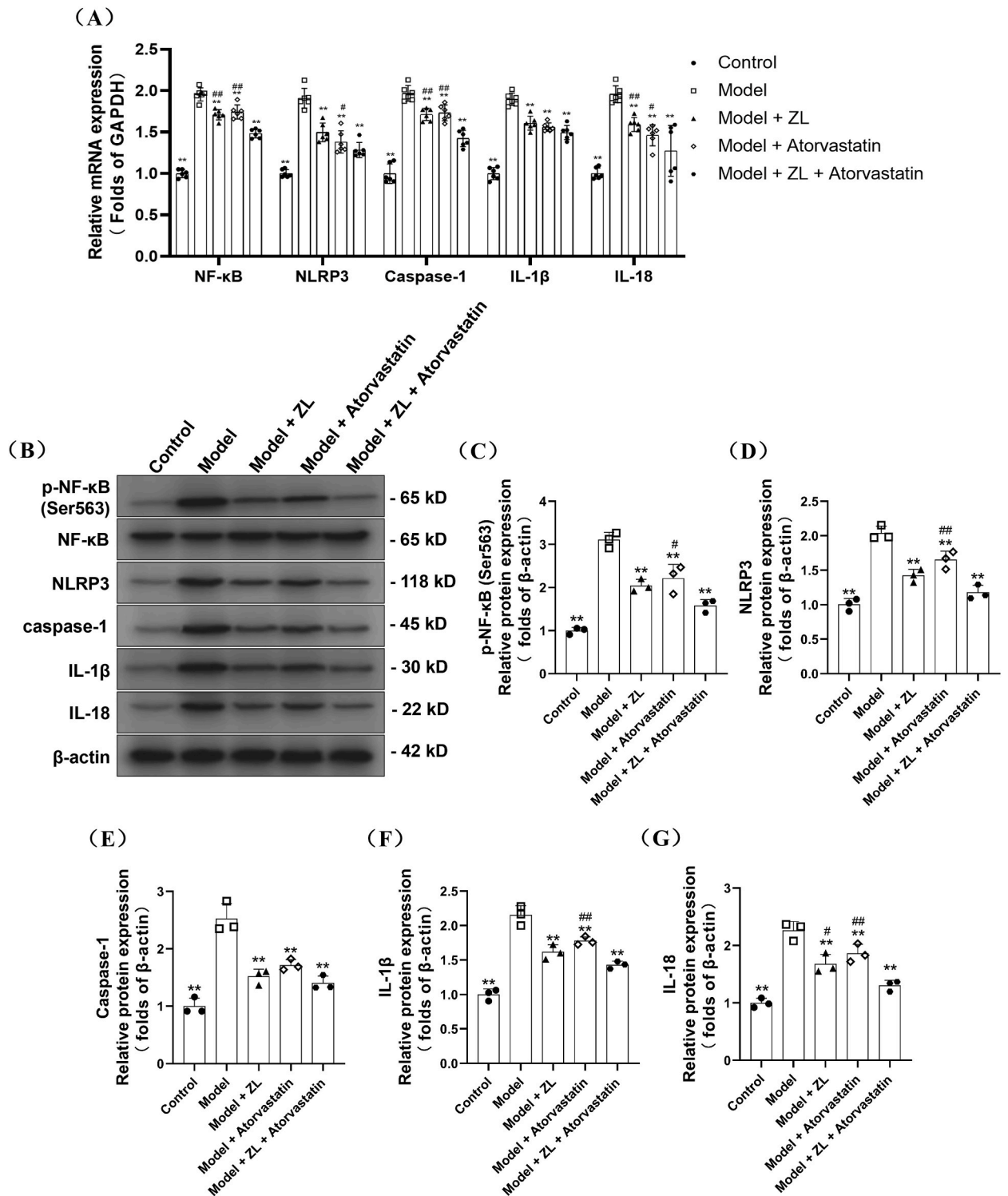


Fig. 5. ZL reduced the mRNA and protein expression levels of inflammatory factors in atherosclerotic tissue. (A) Graphs showed relative expression levels of mRNA, including NF-κB, NLRP3, caspase-1, IL-1β, and IL-18. Bars represent the mean ± SD, n = 6. Western blotting demonstrated ZL downregulated the protein expression of NF-κB/NLRP3 signaling in atherosclerotic tissue. (B) A representative immunoblot, (C) p-NF-κB, (D) NLRP3, (E) caspase-1, (F) IL-1β, (G) IL-18. Bars represent the mean ± SD, n = 3. **p* < 0.05 and ***p* < 0.01 compared to the model group, #*p* < 0.05 and ##*p* < 0.01 compared to the model + ZL + atorvastatin group.

atorvastatin combination, and discussed its possible mechanism from two aspects of lipid infiltration and inflammation.

AS is a chronic inflammatory disease with arterial wall thickening caused by unbalanced lipid metabolism and inappropriate inflammatory response [21]. Cell death is often observed throughout the atherosclerotic process and plays an important role in determining the fate of atherosclerotic lesions. Studies have shown that the cell death in human atherosclerotic plaques involves pyroptosis and apoptosis [22,23]. Pyroptosis is a unique form of cell death that is dependent on Caspase-1 mediation, and is characterized by cell lysis and the release of cytosolic contents into the extracellular space leading to an inflammatory response [24]. Mechanistically, the NLRP3 inflammasome is composed of NLRP3 protein, adaptor protein ASC, and caspase-1. When pro-inflammatory factors stimulate the activation of the inflammasome, ASC plays a role in promoting binding, pro-caspase-1 is cleaved into caspase-1 via proteolytic activity, and caspase-1 cleaves pro-IL-1 β and pro-IL-18, making them active inflammatory factors for amplifying the inflammation cascade reaction [25,26]. Activation of the NLRP3 inflammasome is regulated by multiple signals, such as intracellular potassium efflux, lysosomal disruption, and reactive oxygen species production. Studies have shown that NF- κ B mediates the inflammasome initiation process, and phosphorylated NF- κ B can upregulate the expression of NLRP3 and other related inflammatory factors, which is considered to be one of the main signaling pathways for AS [27–29].

Dyslipidemia is considered a high risk factor for AS, and LDL entering the intima is often modified by ox-LDL, which can induce macrophages and vascular endothelial cells to express adhesion molecules and chemokines, etc., to participate in the inflammatory response [21]. In addition, ox-LDL can induce systemic and local immune responses, and the immune process is regarded as one of the hallmarks of inflammatory responses. LDL-C can be oxidatively modified to activate inflammatory responses and promote AS, whereas HDL-C can transport antioxidant enzymes to terminate lipid oxidation and its inflammatory effects [30–32].

Numerous studies have shown that carotid AS can indirectly reflect the degree and scope of systemic AS, and early detection of carotid AS aids in identifying the risk of future cardiovascular events [33,34]. Intimal media thickness (IMT) is associated with the risk of coronary heart disease and cardiovascular events, and significantly relates to the number and extent of coronary lesions [35–37]. Inflammation of vascular endothelial cells is one of the main reasons for the occurrence of AS [29]. The stress response of the body caused by inflammation promotes the oxidation of low-density lipoprotein, leading to lipid metabolism disorder, reduced clearance function, and damage to the vascular endothelial cells [8]. In addition, hyperlipidemia caused by abnormal lipid metabolism leads to lipid deposition and promotes the formation of intravascular atherosclerotic plaques [21].

Based on the above information, we sorted out the signal pathways and possible pharmacological mechanisms explored in this study, as shown in Fig. 6.

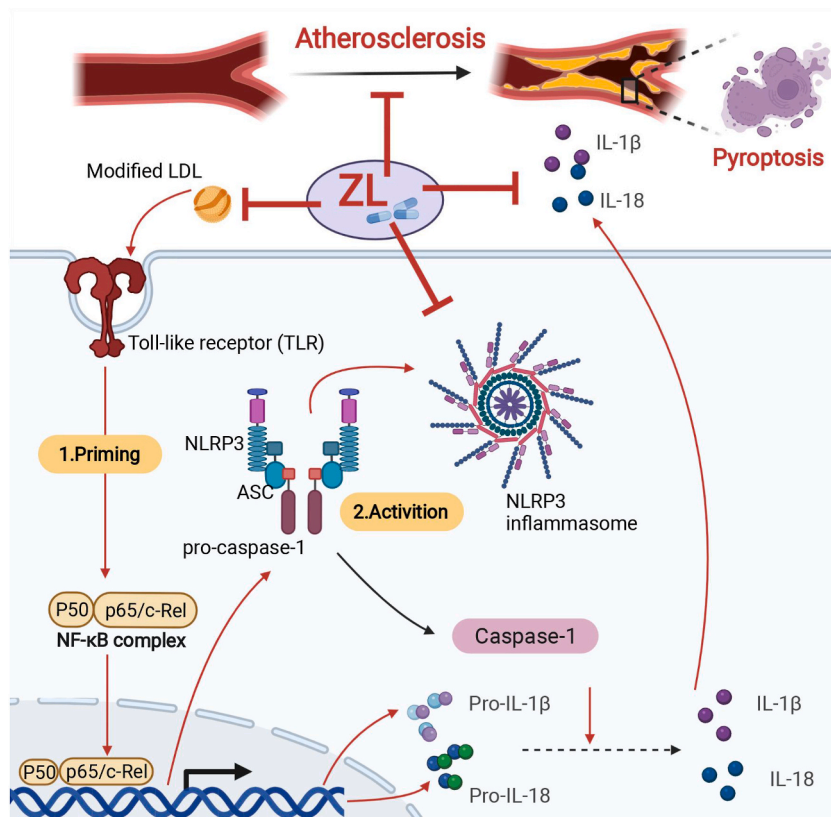


Fig. 6. Zhilong Huoxue Tongyu capsule inhibits hyperlipidemia and AS through NF- κ B/NLRP3 signaling pathway. The graphic was created with BioRender.com.

ZL consists of five drugs, including three herbal medicines and two animal medicines; we performed UPLC-HRMS analysis of these drugs and assessed their pharmacological value [14,15]. Effective active ingredients such as astragaloside IV improve myocardial ischemia and stabilize atherosclerotic plaques [24,38]. The anti-AS activity of cinnamaldehyde is mainly related to the inhibition of inflammatory response [39]. *Caulis Spatholobi* has anti-inflammatory and antioxidant properties [40]. Earthworm extracts have considerable application prospects in the fight against thrombotic diseases [41]. Hirudin extracted from leech is a strong specific inhibitor of thrombin, with anti-fibrinolysis, anti-coagulation, and anti-platelet aggregation effects [42], and the latest research shows that hirudin can inhibit myocardial cell hypertrophy caused by angiotensin II [43]. However, we only listed the role of a few active ingredients, and the interaction between them needs to be confirmed.

In this study, the levels of TG, TC, and LDL-C in the serum of model animals were significantly reduced owing to the intervention of ZL, suggesting that ZL can effectively improve blood lipid metabolism. Histopathological, ZL inhibited the proliferation of smooth muscle cells and the shape of plaques, and protected the vascular endothelium, thereby inhibiting the occurrence and development of AS. Verification of its possible mechanism showed that the mRNA and protein expressions of the core targets of the NF- κ B/NLRP3 signaling pathway were significantly reduced; therefore, the anti-inflammatory effect of ZL can be preliminarily clarified.

At present, statins are the first-line drugs for the clinical treatment of hyperlipidemia and AS [27]. As statins are widely used in clinical practice, the regulation of blood lipids is more scientific and effective, but the risk of AS persists for a long time [44]. has a significant effect on reversing AS and plaque formation, and its mechanism may be anti-inflammatory, and related to lipid regulation and inhibition of smooth muscle cell aggregation [27]. In this study, atorvastatin was selected as the positive control drug to compare with the anti-AS effect of ZL. Notably, in clinical practice, TCMs are often used in combination with modern medicines recommended by clinical guidelines to improve efficacy; our study confirms the rationale of this medication method.

TCM has the advantage of multi-target therapy because it contains a variety of chemical components; however, elucidating the physiological processes of various compounds in the human body is difficult, thereby complicating the explanation of the pharmacological effects of TCM compounds. However, the overall research based on TCM can reveal its scientific connotation to a certain extent [17].

5. Conclusion

ZL significantly reduced blood lipids and inhibited the inflammatory response of blood vessels, and combining it with atorvastatin yielded more optimized efficacy. Our findings have shown that ZL can serve as a new candidate for the treatment of hyperlipidemia and AS. The mechanisms of ZL in pyroptosis, inhibition of inflammatory response, and lipid metabolism need to be studied further.

Ethics statement

Animal experimental procedures were approved by the Animal Research Committee of Southwest Medical University (Approval Number. SWMU20220072). All experimental procedures were performed in accordance with the National Institute of Health Guide for the Care and Use of Laboratory Animals.

Author contribution statement

Mengnan Liu, Raoqiong Wang, Mingtai Chen: Conceived and designed the experiments; Performed the experiments; Analyzed and interpreted the data; Wrote the paper.

Zhongjing Hu, Mei Han: Performed the experiments; Analyzed and interpreted the data.

Maryam Mazhar, Jinyi Xue, Yuan Zou: Contributed reagents, materials, analysis tools or data; Wrote the paper.

Qibiao Wu, Sijin Yang: Contributed reagents, materials, analysis tools or data; Wrote the paper.

Data availability statement

Data will be made available on request.

Funding

This work was supported by the National Natural Science Foundation of China (82074378), Southwest Medical University Project (2021ZKQN143), the Science and Technology Development Fund, Macau SAR (0098/2021/A2), the Science and Technology Planning Project of Guangdong Province (2020B1212030008) and Sichuan Science and Technology Program (2022YFS0618). The funder had no role in the study design, data analysis, or decision to publish.

Declaration of competing interest

The authors declare that they have no known competing financial interests or personal relationships that could have appeared to influence the work reported in this paper.

Acknowledgements

We would like to thank Professor Qibiao Wu and Sijin Yang for their guidance on the research, Mingtai Chen for critical revision of the manuscript, as well as Dr. Zhongjing Hu and Dr. Mei Han for their help in the experiment.

Appendix A. Supplementary data

Supplementary data to this article can be found online at <https://doi.org/10.1016/j.heliyon.2023.e20026>.

References

- [1] G. Qin, L. Luo, L. Lv, Y. Xiao, J. Tu, L. Tao, et al., Decision tree analysis of traditional risk factors of carotid atherosclerosis and a cutpoint-based prevention strategy, *PLoS One* 9 (11) (2017).
- [2] L. Peter, The changing landscape of atherosclerosis, *Nature* (7855) (2021) 592.
- [3] J.F. Polak, D.H. O'Leary, Carotid intima-media thickness as surrogate for and predictor of CVD, *Global Heart* 11 (3) (2016).
- [4] S. Frank, F. Vanessa, K. Johan, L. Esther, Atherosclerosis: the interplay between lipids and immune cells, *Curr. Opin. Lipidol.* 27 (3) (2016).
- [5] S. Kesavardhana, R.K.S. Malireddi, T.-D. Kanneganti, Caspases in cell death, inflammation, and pyroptosis, *Annu. Rev. Immunol.* 38 (1) (2020).
- [6] M. L. S. Y. Z. S. X. B. Q.L. Luo M, S. Yang, Z. Song, X. Bai, Q. Li, Acute toxicity experiment of Zhilong Huoxue Tongyu capsules on mice, *Shizhen Trad Chin Med* 20 (7) (2009) 1639–1640. *Shizhen Trad Chin Med.* 2009;20(07):1639-40.
- [7] X. B. S. Y. M. L. G. L. M.C. Bai X, S. Yang, M. Luo, G. Luo, M. Chen, Long-term toxicity test of Zhilong Huoxue Tongyu capsule on rats, *J Liaoning Univ Trad Chin Med* 12 (2010) 34–37, <https://doi.org/10.13194/j.ljunivtcm.2010.05.36.baix.089>. *Liaoning Univ Trad Chin Med.* 2010;12(05):34-7.
- [8] A.J. Kattoor, N.V.K. Pothineni, D. Palagiri, J.L. Mehta, Oxidative stress in atherosclerosis, *Epub 20170918, Curr. Atherosclerosis Rep.* 19 (11) (2017) 42, <https://doi.org/10.1007/s11883-017-0678-6>. PubMed PMID: 28921056.
- [9] H. Xiao, F. Xuehui, B. Bing, L. Nanjuan, Z. Shuang, Z. Liming, Pyroptosis is a critical immune-inflammatory response involved in atherosclerosis, *Pharmacol. Res.* (2021) 165.
- [10] P. Libby, J.E. Buring, L. Badimon, G.K. Hansson, J. Deanfield, M.S. Bittencourt, et al., *Epub 20190816, Atherosclerosis. Nat Rev Dis Primers.* 5 (1) (2019) 56, <https://doi.org/10.1038/s41572-019-0106-z>. PubMed PMID: 31420554.
- [11] X. Suowen, I. Iqra, J. Lp, L. Hong, K. Danielle, Z. Xueying, et al., Endothelial dysfunction in atherosclerotic cardiovascular diseases and beyond: from mechanism to pharmacotherapies, *Pharmacol. Rev.* 73 (3) (2021).
- [12] L. Ting-Ting, W. Zhi-Bin, L. Yang, C. Feng, Y. Bing-You, K. Hai-Xue, The mechanisms of traditional Chinese medicine underlying the prevention and treatment of atherosclerosis, *Chin. J. Nat. Med.* 17 (6) (2019) 401–412.
- [13] E.L.-H. Leung, S. Xu, Traditional Chinese medicine in cardiovascular drug discovery, *Pharmacol. Res.* (2020) 160.
- [14] P. Liang, L. Mao, Y. Ma, W. Ren, S. Yang, A systematic review on Zhilong Huoxue Tongyu capsule in treating cardiovascular and cerebrovascular diseases: pharmacological actions, molecular mechanisms and clinical outcomes, *Epub 20210524, J. Ethnopharmacol.* 277 (2021), 114234, <https://doi.org/10.1016/j.jep.2021.114234>. PubMed PMID: 34044079.
- [15] M. Maryam, Y. Guoqiang, M. Linshen, L. Pan, T. Ruizhi, W. Li, et al., Zhilong Huoxue Tongyu capsules ameliorate early brain inflammatory injury induced by intracerebral hemorrhage via inhibition of canonical NFκB signalling pathway, *Front. Pharmacol.* 13 (2022).
- [16] L. Mengnan, L. Gang, L. Tianzhu, Y. Tingfu, W. Raoqiong, R. Wei, et al., Zhilong Huoxue Tongyu capsule alleviated the pyroptosis of vascular endothelial cells induced by ox-LDL through miR-30b-5p/NLRP3, in: *Evidence-Based Complementary and Alternative Medicine*, 2022, p. 2022.
- [17] C. Wang, M. Niimi, T. Watanabe, Y. Wang, J. Liang, J. Fan, Treatment of atherosclerosis by traditional Chinese medicine: questions and quandaries, *Atherosclerosis* 277 (2018).
- [18] C. Xing, R. Song, G. Mm, D. Sudharshan, L. Lin, X. Mengzhou, et al., Hirulog-like peptide reduces restenosis and expression of tissue factor and transforming growth factor-beta in carotid artery of atherosclerotic rabbits, *Atherosclerosis* 169 (1) (2003).
- [19] B. Emini Veseli, P. Perrotta, G.R.A. De Meyer, L. Roth, C. Van der Donckt, W. Martinet, et al., Animal models of atherosclerosis, *Epub 20170505, Eur. J. Pharmacol.* 816 (2017) 3–13, <https://doi.org/10.1016/j.ejphar.2017.05.010>. PubMed PMID: 28483459.
- [20] S. Yang, C. Wang, B. Xue, G. Luo, H. Pan, Effect of Yiqi qufeng Tongluo method on the expression of NF-κB and ICAM-1 in hypertensive carotid atherosclerosis rabbits, *Journal of Luzhou Medical College* 37 (1) (2014) 47–51.
- [21] F. Tu, Hyperlipidemia and cardiovascular disease: inflammation, dyslipidemia, and atherosclerosis, *Curr. Opin. Lipidol.* 25 (1) (2014).
- [22] Y.J. Xu, L. Zheng, Y.W. Hu, Q. Wang, Pyroptosis and its relationship to atherosclerosis, *Epub 20171110, Clin. Chim. Acta* 476 (2018) 28–37, <https://doi.org/10.1016/j.cca.2017.11.005>. PubMed PMID: 29129476.
- [23] Q. Zhengtao, Z. Yilin, W. Chuandan, D. Yimai, Z. Yaoyao, X. Yeqiong, et al., Pyroptosis in the initiation and progression of atherosclerosis, *Front. Pharmacol.* 12 (2021).
- [24] C. Jia, H. Chen, J. Zhang, K. Zhou, Y. Zhuge, C. Niu, et al., Role of pyroptosis in cardiovascular diseases, *Epub 20181217, Int. Immunopharm.* 67 (2019) 311–318, <https://doi.org/10.1016/j.intimp.2018.12.028>. PubMed PMID: 30572256.
- [25] H. Zahra, S. Fatemeh, R. Bahman, S. Amirhossein, M. Aria, M. Hamed, NLRP3 inflammasome: its regulation and involvement in atherosclerosis, *J. Cell. Physiol.* 233 (3) (2018).
- [26] B. Magnus, Y. Arif, T. Ira, Ö. Katariina, T. Kp, Inflammation and its resolution in atherosclerosis: mediators and therapeutic opportunities, *Nat. Rev. Cardiol.* 16 (7) (2019).
- [27] K. Koushki, S.K. Shahbaz, K. Mashayekhi, M. Sadeghi, Z.D. Zayeri, M.Y. Taba, et al., Anti-inflammatory action of statins in cardiovascular disease: the role of inflammasome and Toll-like receptor pathways, *Clin. Rev. Allergy Immunol.* 60 (2) (2021) 175–199, <https://doi.org/10.1007/s12016-020-08791-9>. PubMed PMID: 32378144; PubMed Central PMCID: PMC7985098.
- [28] S. Sivanan, W. Naruemon, T. Jiraporn, C. Waraluck, S. Apichart, T. Chainarong, Pelargonic acid vanillylamide and rosuvastatin protect against oxidized low-density lipoprotein-induced endothelial dysfunction by inhibiting the NF-κB/NLRP3 pathway and improving cell-cell junctions, *Chem. Biol. Interact.* 345 (2021).
- [29] S. Xu, H. Chen, H. Ni, Q. Dai, Targeting HDAC6 attenuates nicotine-induced macrophage pyroptosis via NF-κB/NLRP3 pathway, *Epub 20201124, Atherosclerosis* 317 (2021) 1–9, <https://doi.org/10.1016/j.atherosclerosis.2020.11.021>. PubMed PMID: 33321327.
- [30] M. Winfried, E. Km, S. Hubert, S. Timotheus, Z. Stephen, R. Andreas, et al., HDL cholesterol: reappraisal of its clinical relevance, *Clin. Res. Cardiol. : official journal of the German Cardiac Society* 106 (9) (2017).
- [31] R. Anand, W. Marit, vE. Arnold, R. Alan, R.K. Anne, HDL in the 21st century: a multifunctional roadmap for future HDL research, *Circulation* 143 (23) (2021).
- [32] Z. Evangelia, K.D. Sotiria, V. Aggeliki, X. Eva, A. Ke, H. Aikaterini, et al., High density lipoprotein in atherosclerosis and coronary heart disease: where do we stand today? *Vasc. Pharmacol.* (2021) 141.
- [33] M. vMACC, P. Sjaak, W. Jelmer, C. Wm, J. Tdh, Carotid artery reactivity predicts events in peripheral arterial disease patients, *Ann. Surg.* 269 (4) (2019).

- [34] B. Daniel, A. Banafsheh, J.A. vdBQ, I.M. Kamran, S. Mariana, W. Vm, et al., Atherosclerotic carotid plaque composition and incident stroke and coronary events, *J. Am. Coll. Cardiol.* 77 (11) (2021).
- [35] Y.S. Ali, K.E. Rembold, B. Weaver, M.B. Wills, S. Tatar, C.R. Ayers, et al., Prediction of major adverse cardiovascular events by age-normalized carotid intimal medial thickness, *Atherosclerosis* 187 (1) (2005).
- [36] L. Da, F. Bb, Carotid intima-media thickness testing as an asymptomatic cardiovascular disease identifier and method for making therapeutic decisions, *Postgrad. Med.* 125 (2) (2013).
- [37] Y. YuChun, F. KaiMin, H. WanLun, L. LiJen, The effectiveness of high-resolution ultrasound in the assessment of the carotid intima-media thickness for postirradiated neck, *Eur. Arch. Oto-Rhino-Laryngol. : official journal of the European Federation of Oto-Rhino-Laryngological Societies (EUFOS) : affiliated with the German Society for Oto-Rhino-Laryngology - Head and Neck Surgery* 276 (4) (2019).
- [38] N. Wang, X. Zhang, Z. Ma, J. Niu, S. Ma, W. Wenjie, et al., Combination of tanshinone IIA and astragaloside IV attenuate atherosclerotic plaque vulnerability in ApoE(-/-) mice by activating PI3K/AKT signaling and suppressing TLR4/NF- κ B signaling, *Biomed. Pharmacother.* 123 (C) (2020).
- [39] L. Weifeng, Z. Wenbing, Z. Jimmeng, L. Wenqi, Z. Lulu, L. Fang, et al., Cinnamaldehyde attenuates atherosclerosis via targeting the I κ B/NF- κ B signaling pathway in high fat diet-induced ApoE(-/-) mice, *Food Funct.* 10 (7) (2019).
- [40] P. Tang, H. Liu, B. Lin, W. Yang, W. Chen, Z. Lu, et al., *Spatholobi Caulis* dispensing granule reduces deep vein thrombus burden through antiinflammation via SIRT1 and Nrf2, *Phytomedicine* 77 (2020).
- [41] K. Essam, The biotechnological potential of fibrinolytic enzymes in the dissolution of endogenous blood thrombi, *Biotechnol. Prog.* 30 (3) (2014).
- [42] J. Chen, X. Xie, H. Zhang, G. Li, Y. Yin, X. Cao, et al., Pharmacological activities and mechanisms of hirudin and its derivatives - a review, *Front. Pharmacol.* 12 (2021).
- [43] L. Mengnan, L. Gang, D. Li, M. Maryam, W. Li, H. Wenlu, et al., Network pharmacology and in vitro experimental verification reveal the mechanism of the hirudin in suppressing myocardial hypertrophy, *Front. Pharmacol.* 13 (2022).
- [44] D.S. Kazi, J.M. Penko, K. Bibbins-Domingo, Statins for primary prevention of cardiovascular disease: review of evidence and recommendations for clinical practice, *Med. Clin.* 101 (4) (2017).